Springer

KSME

Journal of Mechanical Science and Technology 26 (1) (2012) 123~128
www.springerlink.com/content/1738-494x
DOI 10.1007/s12206-011-0936-4

Modeling and computation of the three-roller bending process of steel sheets †

Ahmed Ktari*, Zied Antar, Nader Haddar and Khaled Elleuch

Unité de Recherche de Chimie Industrielle et Matériaux, ENIS, BP W, 3038-1173 Sfax, Tunisie

(Manuscript Received July 9, 2010; Revised December 13, 2010; Accepted September 18, 2011)

Abstract

Sheet metal bending processes are some of the most commonly used industrial manufacturing operations. The development and optimization of these processes are time consuming and costly. Therefore, finite element simulations may aid the design and quality assurance of sheet metal products. In the present study, a commercial finite element package was used to analyze the three-roller bending of a steel sheet. A two-dimensional finite element model of this process was built under the ABAQUS/Explicit environment based on the solution of several key techniques, such as contact boundary condition treatment, material property definition, meshing technique, and so on. Maps with desired curvature radii were established by varying the distance between the two bottom rollers and the position of the upper one. The developed maps made the rolling process easier and less time consuming. An industrial experiment using optimized numerical results was carried out to validate the numerical model. Residual stress and equivalent plastic strain distributions were also studied. The numerical spring back phenomenon was compared with analytical results.

Keywords: Cylindrical bending; Finite elements analysis; Residual stress; Spring back

1. Introduction

Cylindrical sections or ferrules are used in many engineering applications like pressure vessels, heat-exchanger shells, and boiler chambers. They also form the major skeleton of oil and gas rigs. Rolling machines with both three and four rolls are indispensable to the production of ferrules with various curvatures [1-3]. To date, research on the cold cylindrical bending process has been done using only analytical and empirical models. Yang and Shima [4] have discussed the distribution of curvature and calculated bending moment in accordance with the displacement and rotation of rolls by simulating the deformation of a workpiece with a U-shaped cross-section in a three-roller bending process. Hua et al. [3] have proposed a formulation to determine the bending force on rollers, the driving torque, and the power in the continuous single-pass four-roll bend of thin plate. Gandhi and Raval [5] have developed analytical and empirical models to estimate explicitly the top roller position as a function of the final radius of curvature for the three-roller cylindrical bending of plates.

In the present paper, the three-roller bending process parameters were studied using two-dimensional dynamic explicit finite element (FE) analysis. As schematically shown in Fig. 1, the sheet metal was fed by two side rollers from point A, bent to an arbitrary curvature by adjusting the position of the top roller, and then exited at point B. Afterwards, the workpiece was welded together to produce a ferrule. The rolling process always began with the crucial operation of pre-bending both ends of the workpiece (Fig. 2). This operation eliminated flat spots when rolling a full cylindrical shape and ensured better closure of the seam.

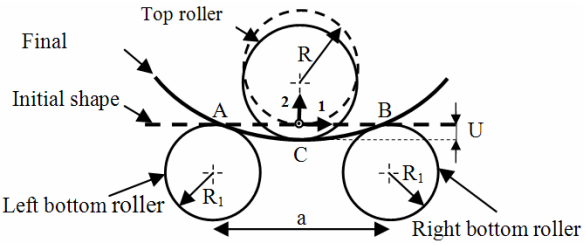

Fig. 1. Configuration of a pyramidal three-roller bending machine.

Fig. 2. Initial dimensions of the workpiece for modeling (in mm).

The success of the three-roller bending process heavily depends on the experience and skill of the operator. The work-

† This paper was recommended for publication in revised form by Associate Editor Youngseog Lee

* Corresponding author. Tel.: +216 22 67 62 08
E-mail address: ahmedingmat@yahoo.fr

piece bend is generally produced via the multi-pass method, also named "trial and error" to optimize the bending capacity of the roller benders. Nevertheless, the multi-pass method suggests high costs owing to material wastage and loss of production time. The repeatability, precision, and productivity of the process require the use of a single-pass production method [5].

However, the latter method has been always a challenge because an operator must have knowledge of the different machine parameters to obtain ferrules with desired diameter. The parameters include the position of the top roller (U), distance between the bottom rollers (a), and thickness of the sheet metal (e).

2. FE modeling

The rolling process is complicated from an FE modeling perspective. Its common features with other forming processes include large strain plasticity, large displacements, and contact phenomena. However, this process seems to be more complicated than other forming processes. For instance, the workpiece is pulled into the roll gap by friction due to the motions of the upper and lower rollers.

To model the rolling process using Abaqus FEs code and to ensure the accuracy and efficiency of computation, many key techniques were taken into account, such as geometry modeling, assembling, treating of contact boundary conditions, definition of material properties, mesh, and so on [6]. These techniques are detailed in the next section.

2.1 Modeling problem

Both implicit and explicit solution methods were tried to run successful simulations. The implicit method is favorable in models where large time increments can be used. Several attempts using the implicit method were made, but simulations were interrupted after a few rotation degrees. Given the nonlinearity of the problem and the severe contact conditions, using large time increments was not possible. Consequently, the explicit solution method seemed more suitable because very small time increments were needed in the problem. This choice of the dynamic explicit procedure has been confirmed by Han and Hua [7] using a model of the cold rotary forging process of a ring workpiece. The explicit dynamic analysis procedure was based on the implementation of an explicit integration rule using diagonal element mass matrices. The equations of motion for the body were integrated using the explicit central-difference integration rule [8], as shown in the following:

$$\dot{u}^{N}_{\left(i+\frac{1}{2}\right)} = \dot{u}^{N}_{\left(i-\frac{1}{2}\right)} + \frac{\Delta t_{(i+1)} + \Delta t_{(i)}}{2} \ddot{u}^{N}_{(i)} \quad , \tag{1}$$

$$u^{N}_{(i+1)} = u^{N}_{(i)} + \Delta t_{(i+1)} \dot{u}^{N}_{\left(i+\frac{1}{2}\right)} \tag{2}$$

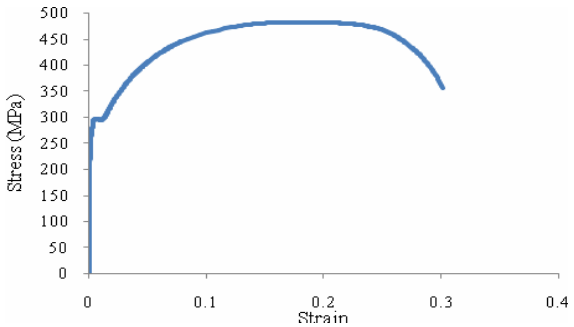

Fig. 3. Uniaxial tensile tests of S275JR.

where u^N is a degree of freedom and the subscript i refers to the increment number in an explicit dynamic step.

The different steps are detailed in the following sections.

2.2 Modeling problem

The entire three-roller bending process model was made up of a workpiece and rollers. The sheet steel was defined as a deformable body, and the rollers, which were not deformable, were defined as discrete rigid bodies. Each of these rigid bodies was assigned to a reference point (RP) to represent its rigid motion in all degrees of freedom.

2.3 Material properties

The rollers were made from C46-forged carbon steel, and were presumed to be rigid bodies. A steel sheet was assigned as a deformable body. The material properties of S275JR steel were defined using Young's modulus E, density ρ, and Poisson's ratio v. To determine the plastic behavior of the steel, a conventional stress-strain curve was obtained from a uniaxial tensile test (NF A 03-151), as presented in Fig. 3. Isotropic elasticity behavior was assumed, with Young's modulus of 210 GPa and Poisson's ratio of 0.3. Strain hardening was described using several points of tensile stress versus plastic strain over the yield strength (290 MPa) and below the tensile strength (489 MPa). The dynamic explicit method was used in the computation, and the weight of the sheet was taken into account. The steel density used was 7800 $kg \cdot m^{-3}$. Mass scaling greatly affects computational results; a greater is the mass scaling the shorter is the computation time. However, very high mass scaling can lead to an unstable solution. In the present work, the optimized mass scaling parameter was found to be 3000 times.

2.4 Contact definition

The finite element code Abaqus uses surfaces to describe contacts and interactions between different parts of a rolling machine. A master–slave contact approach is used in an analysis where the rollers are considered as the master surfaces, and the sheet surfaces facing the rollers constitute the

Table 1. Friction parameters between different surfaces.

	Top roller (C46) – steel sheet (S275JR)	Bottom rollers (C46) – steel sheet (S275JR)
Friction coefficient (bending)	0.2	0.2
Friction coefficient (rolling)	1	0.2

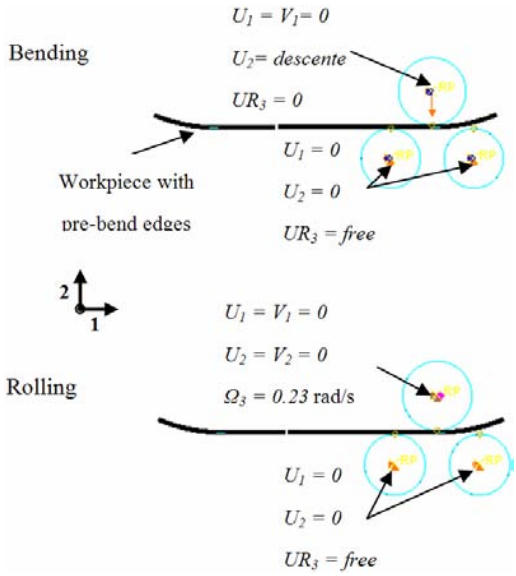

Fig. 4. Applied loads and boundary conditions.

slaves. In the present study, the interaction between the workpiece and tools (upper and bottom rollers) was formulated using the finite sliding approach, which allowed the possibility of separating the surfaces during the rolling operation. The friction on the contact surfaces was assumed to meet the Coulomb friction law. All friction coefficients were also assumed to be constant during the rolling process (Table 1).

2.5 Constraints and load definition

All constraints and loads in the three-roller bending analysis model were referenced to the global coordinate system. The process model was achieved in two steps. The first was the sheet bending, or simply "bending." The second was the circular deformation of the sheet, called "rolling." The rigid motions of the rollers were represented by their RPs. Hence, the constraints and loads applied on the rollers were exerted on their RPs. Boundary conditions and loading were carried out through the two modes of displacement/rotation and velocity/angular velocity (Fig. 4). During the first step, the bottom rollers were free to rotate only about the global X3-axis, whereas the upper roller was constrained to translate only along the global X2-axis. In the second step, the upper roller rotated around the X3-axis with an angular velocity of 0.23 rad·s^{-1}, whereas, the bottom rollers remained within the same boundary condition as defined in the previous step.

Fig. 5. Comparison of numerical and experimental results (diameter = 1000 mm).

2.6 Meshing techniques

Element types, the number of elements, and mesh quality are important in meshing technologies. The workpiece was discretized by reducing the integration linear plane stress (CPS4R) elements. The rollers were meshed using rigid linear (R2D2) elements. The elements types used were available in the ABAQUS element library.

3. Modeling validation

To validate the finite element model of the three-roller bending process, the experimental and numerical results were compared. Several computations were realized by varying the top roller position and maintaining the distance between the bottom rollers at 750 mm. The computations were performed using the dynamic procedure in the ABAQUS/explicit code. The CPU time calculated with a 3 GHz processor was about 450 min with the model containing more than 6900 elements, which corresponded to 15 500 degrees of freedom. A three-roller bending machine was equipped with the appropriate instrumentation needed to set the distance between the bottom roller centers and the position of the upper roller. For this industrial test, process parameters were provided by the simulation. Fig. 5 compares the numerical and experimental results. Indeed, optimized parameters allowed for obtaining the same diameter from the real and theoretical cases. Hence, the accuracy of the simulation was verified.

4. Results and discussion

Fig. 6 shows the different steps in the rolling process obtained via numerical computation. Clearly, the distribution of the curvature was asymmetric at about the top contact point (between the top roller and sheet). This finding, which can be explained by the asymmetrical deformation about the maximum bending moment point, well agreed with that of Yang and Shima [4] as well as Yang et al. [9]. The workpiece thickness also remained constant after the bending and rolling processes.

4.1 Residual stress and plastic strain distribution

The distributions of residual stress and equivalent plastic

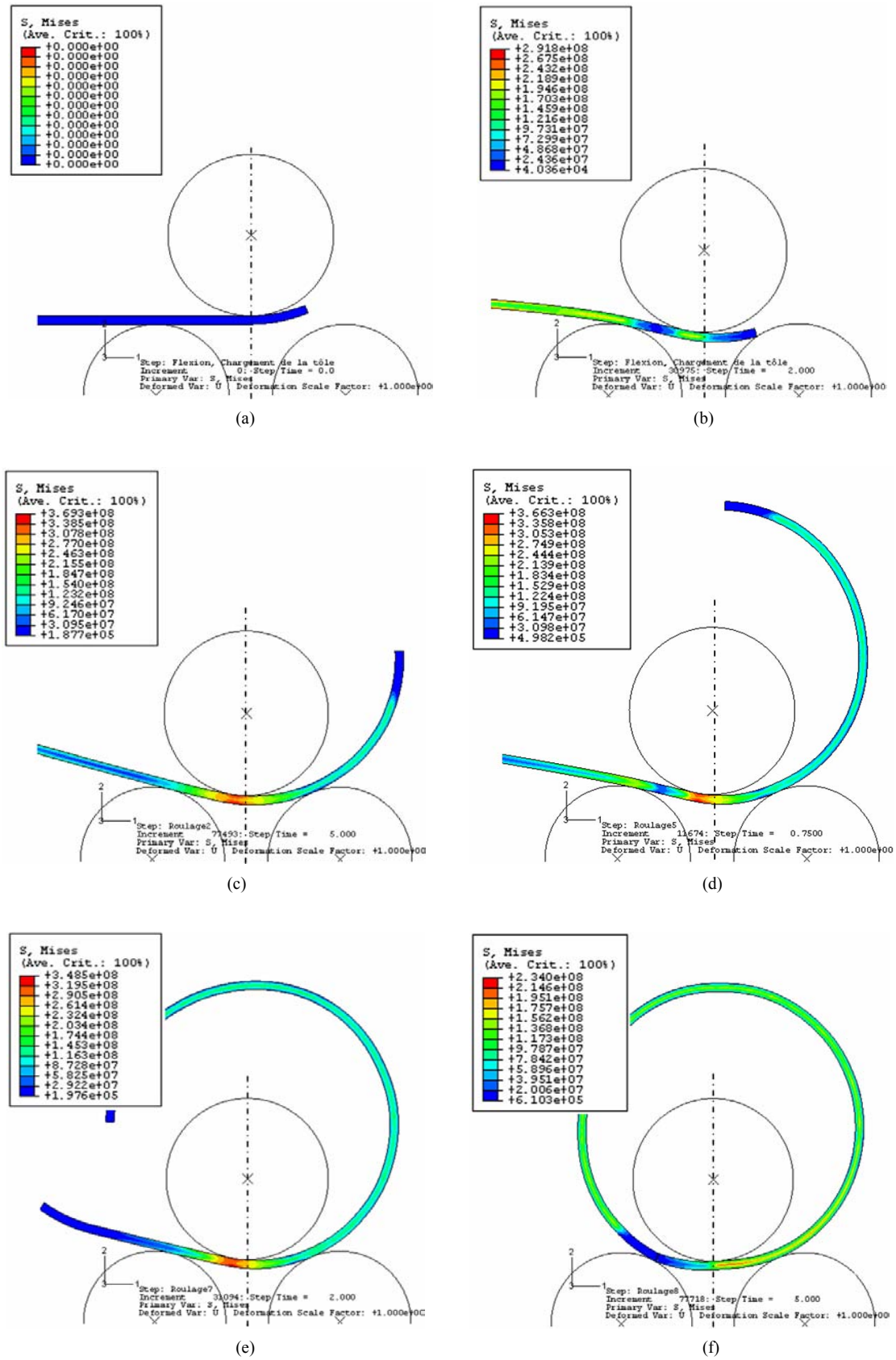

Fig. 6. Cylindrical rolling process phases: (a) initial bending condition; (b) initial rolling condition; (c) ¼ of the rolling process; (d) ½ of the rolling process; (e) ¾ of the rolling process; (f) obtained ferrule.

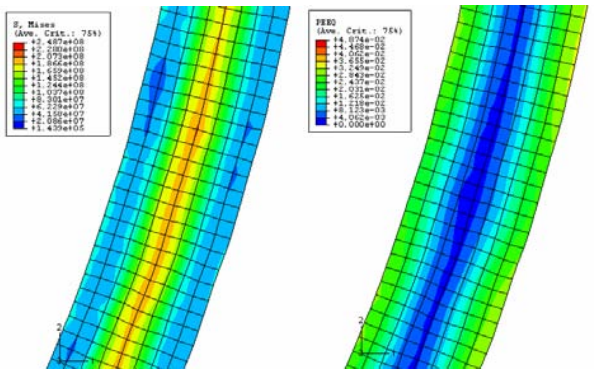

Fig. 7. Distribution of (a) residual stress; (b) equivalent plastic strain over a section of bend.

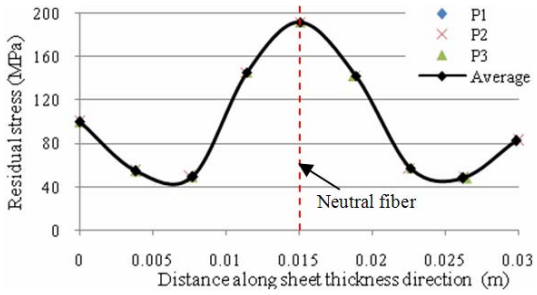

Fig. 8. Distribution of the residual stress along the sheet thickness at three different positions on formed ferrule (P1, P2, and P3).

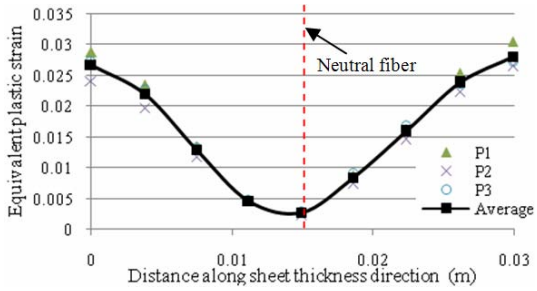

Fig. 9. Distribution of the equivalent plastic strain along the sheet thickness at three different positions on formed ferrule (P1, P2, and P3).

strain on the bend sheet part (Figs. 7 and 8) indicated that the maximum residual stress was located in the vicinity of neutral fiber with a value of 190 MPa. The distance from the neutral fiber increased, whereas the residual stress continuously decreased until reaching a value of 50 MPa at 6 mm from the sheet surfaces. Figs. 7 and 9 show the distribution of equivalent plastic strain over sheet thickness. The maximum plastic strain was located on ferrule surfaces, and the minimum value was in the neutral fiber zone. These results were consistent with those obtained by Bouhêlier [10].

4.2 Establishment of rolling maps

After validating the three-roller bending process model,

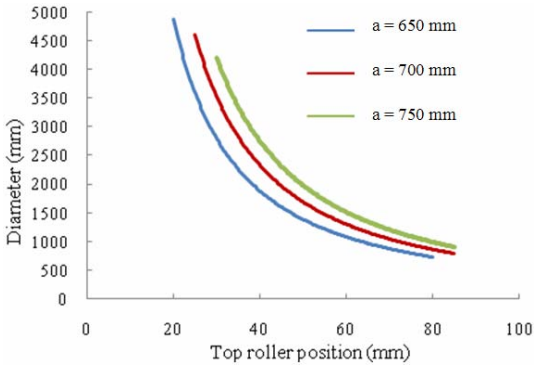

Fig. 10. Final diameter (mm) versus top roller position (mm) and the center distance between the bottom rollers (mm) with a sheet thickness of about 14 mm.

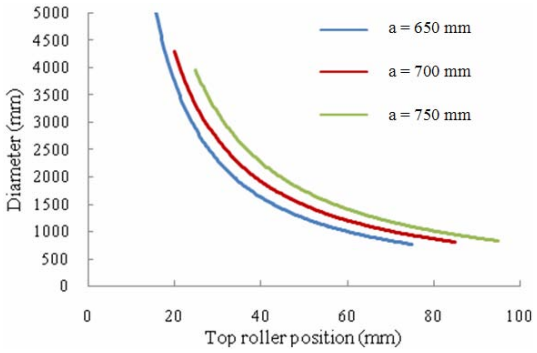

Fig. 11. Final diameter (mm) versus top roller position (mm) and the center distance between the bottom rollers (mm) with a sheet thickness of about 30 mm.

several computations were performed with various top roller positions (U) to obtain ferrules with final diameters ranging from 800 to 4000 mm. This approach was repeated for different distances between the bottom rollers (a). Figs. 10 and 11 show that lower top roller positions resulted in higher diameters. Longer distances between the bottom rollers also resulted in bigger ferrule diameters when the distance of the top roller position was constant. This result well agreed with that of Gandhi and Raval [5], who have studied the effect of the top roller position (U) on the desired curvature radius (R_f).

4.3 Spring back in formed sheet metal

In the rolling process, the radius through which the sheet steel is bent must be smaller than the required radius because of the spring back phenomenon. The amount of spring back depends on several materials and such machine properties as the elasticity modulus, shape of the stress-strain curve, sheet thickness, roller dimensions, and so on. To study the spring back phenomenon produced on steel sheets, the rolling process is often used. The evolution of the initial curvature radius R_0 versus the obtained radius R_f (normed by sheet thickness) was established (Fig. 12). The first curve was obtained by numerical simulation of the rolling process. The second was

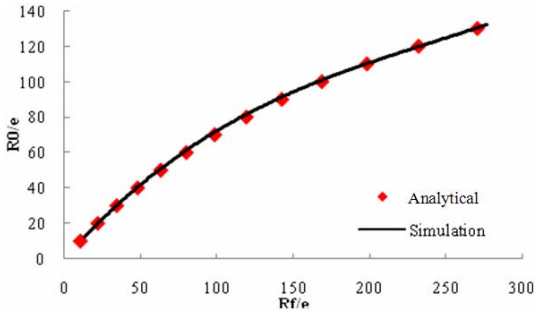

Fig. 12. Comparison between the analytical and numerical spring back distance between the bottom rollers 650 mm (material tensile strength = 292 MPa).

determined by Bouhêlier [10] using empirical Eq. (3).

$$R_f = \frac{R_0}{1 - \frac{3}{2}\left[2\left(\frac{R_0}{e}\right)\left(\frac{\sigma_y}{E}\right)\right] + \frac{1}{2}\left[2\left(\frac{R_0}{e}\right)\left(\frac{\sigma_y}{E}\right)\right]^3}, \quad (3)$$

where E, σ_y, and e are the Young's modulus, yield stress, and sheet thickness, respectively.

Fig. 12 shows that the numerical and analytical spring back values were in good agreement. However, Bouhêlier [10] has assumed that the material has a perfect elasto-plastic behavior. This behavior can be explained by the low plastic strain value (between 0.2% and 3.2%), as previously observed (Fig. 9).

5. Conclusions

A mechanical dynamic analysis of steel sheet bending with a three-roller machine was performed using the Abaqus/ Explicit code. First, the modeling was validated by comparing the numerical and experimental results. Several maps were then developed, enabling variations in desired ferrule diameters versus positions of the top roller and the distance between the bottom rollers of both 14 and 30 mm sheet thicknesses. Maps made the rolling process easier and faster. The residual stress and plastic strain through the workpiece thickness were estimated. Finally, the spring back obtained with the FE results were compared with an analytical solution obtained in a similar study on the three-roller bending process. This comparison showed that the numerical and analytical results were in good agreement.

References

[1] M. Hua, D. H. Sansome, K. P. Rao and K. Baines, Continuous four-roll plate bending process: Its bending mechanism and influential parameters, *Journal of Materials Processing Technology,* 45 (1994) 181-186.

[2] M. Hua, K. Baines and I. M. Cole, Bending mechanisms, experimental techniques and preliminary tests for the continuous four-roll plate bending process, *Journal of Materials Processing Technology,* 48 (1995) 159-172.

[3] M. Hua, I. M. Cole, K. Baines and K. P. Rao, A formulation for determining the single-pass mechanics of the continuous four-roll thin plate bending process, *Journal of Materials Processing Technology,* 67 (1997) 189-194.

[4] M. Yang and S. Shima, Simulation of pyramidal type three-roller bending process, *Int. J. Mech. Sci.,* 30-12 (1988) 877-886.

[5] A. H. Gandhi and H. K. Raval, Analytical and empirical modeling of top roller position for three-roller cylindrical bending of plates and its experimental verification, *Journal of materials processing technology,* 197 (2008) 268-278.

[6] G. Y. Zhao, Y. L. Liu, H. Yang, C. H. Lu and R. J. Gu, Three-dimensional finite-elements modeling and simulation of rotary-draw bending process for thin-walled rectangular tube, *Materials Science and Engineering A,* 499 (2009) 257-261.

[7] X. Han and L. Hua, 3D FE modeling of cold rotary forging of a ring workpiece, *Journal of Materials Processing Technology,* 209 (2009) 5353-5362.

[8] H. Karlsson, *Abaqus/CAE user's manuel*, version 6.4, Abaqus, Inc, 2007.

[9] M. Yang, S. Shima and T. Watanabe, Model base control for three roller bending process of channel bar, Eng. Ind. Trans. ASME, 112 (1990) 346-351.

[10] C. Bouhêlier, *Formage des tôles fortes*, Techniques ingénieurs, B 7630 (1982) 5-19 (in french).

Ahmed Ktari received an engineering diploma in materials engineering from the National Engineering School of Sfax (ENIS) in 2007. He is currently a Ph.D student in materials science and engineering at ENIS. His major topics of interest include fatigue and fracture, mechanical behavior of materials, and FE analysis problems.

Zied Antar obtained his engineering diploma in materials engineering from the National Engineering School of Sfax (ENIS) in 2007. He finished a master course in the eco-conception of polymer and composites at the South-Brittany University (UBS) in 2008. He is presently a Ph.D student. His main research is on the eco-conception of conductive polymer composites for energy production and storage.